# Chemical-bonding aspects of heterogeneous catalysis II : solid acids

# Recueil Review

of progress in current research

## Chemical-bonding aspects of heterogeneous catalysis. II. Solid acids

**R. A. van Santen**

*Koninklijke/Shell-Laboratorium (Shell Research B.V.), Amsterdam, The Netherlands*
*(Received December 10th, 1981)*

### 1. Introduction

We have seen in the previous paper[1] that the degree of coordinative unsaturation of surface atoms is an important variable and chemisorption is visualized to comprise three steps: localization of electrons, complex formation and readsorption.
It is interesting that this description valid for the formation of covalent electron bonds between metal surface and adsorbing molecule, bears a close resemblance to chemisorption on solid acids involving protons:

$$AH + M \rightarrow A^- + MH^+$$

The protonation energy can be decomposed into three components[2]:

$$E_{proton} = E_{solv} + E_{add} - E_{diss}$$

where $-E_{diss}$ is the energy cost of dissociating the AH bond, $E_{add}$ is the energy gain of protonating M and $E_{solv}$ is the solvation energy of $MH^+$ due to its adsorption on the ionized solid acid surface. As we will demonstrate, one can only understand differences between solid acids, if all three components are accounted for. We will discuss the acidic properties of clays using recent experimental results and present an analysis of electrovalent chemisorption based on purely electrostatic interactions.
As in the previous paper[1] it is of interest to pose the question whether or not adsorption is purely local. It will be shown that differences in acidity between zeolites and clays cannot be understood if adsorption is considered to be purely local, as they are related to differences in Madelung potentials.
A simple method to estimate the degree of coordinative unsaturation at an ionic surface is the use of *Pauling*'s electrostatic valencies[3]. Let $Z$ be the formal electric charge or valence of a cation and $\nu$ its coordination number. The strength of the electrostatic bond to each coordinated anion is: $s = Z/\nu$. According to Pauling in a stable ionic structure the formal charge $Z$ of each anion or cation is, with changed sign, exactly or nearly exactly equal to the sum of the strength of the electrostatic bonds to it from the adjacent cations or anions ($\zeta^{\mp}$):

$$-Z = \zeta = \sum_i s_i = \sum_i \frac{Z_i}{\nu_i}$$

The summation is taken over the cations at the centres of all the polyhedra of which the anion forms a corner. So the electrostatic bond strength is purely a local parameter. Application to clay and zeolite solid acids will show the use, but also the limitation of this approach. We will first illustrate the application of *Pauling*'s electrostatic valencies by discussing the $Al_2O_3$ and $SiO_2$ surfaces.
In bulk corundum $Al^{3+}$ is octahedrally coordinated to six $O^{2-}$ ions. Each anion shares six octrahedra. Four contain an $Al^{3+}$ cation, One derives:

$$s_{Al} = \frac{+3}{6} = +\frac{1}{2}; \quad s_O = \frac{-2}{4} = -\frac{1}{2}$$

$$\zeta_{Al} = 6 \times -\frac{1}{2} = -3; \quad \zeta_O = 4 \times \frac{1}{2} = 2$$

So *Pauling*'s valence rule is obeyed. A surface is preferentially formed in such a way that the change in coordination number of cations and anions is as small as possible. At a surface the sum of positive and negative unsaturated valencies has to be zero because electrostatic neutrality has to be maintained. The unsaturated valency is defined as:

$$v^{\pm} = Z^{\pm} + \zeta^{\pm}$$

The unsaturated valencies can be considered a measure for the acidity or basicity of an ionic surface. For the particular case of $Al_2O_3$ the face of lowest surface energy contains $O^{2-}$ and $Al^{3+}$ that have lost one of their neighbours in the first coordination shell. So the unsaturated valencies are:

$$v^+ = +\frac{1}{2}$$

When $H_2O$ is adsorbed to the surface Brønsted acid and basic sites are created. The $OH^-$ adsorbs onto the $Al^{3+}$ ion, which now gets as value for $v$:

$$v^+ = -\frac{1}{2}$$

The proton adsorbs onto the $O^{2-}$ ion, and $v^-$ becomes:

$$v^- = +\frac{1}{2}$$

The Lewis acid site is converted into a basic site, and the Lewis basic site becomes acidic.

---

1. *R. A. van Santen*, Recl. Trav. Chim. Pays-Bas **101**, 121 (1982).
2. *V. B. Kasanski*, Bulgarian Academy of Sciences, Communications of the Department of Chemistry **13**, 19 (1980).
3. *L. Pauling*, "The Nature of the Chemical Bond", Cornell University Press, 1960; p. 548, 549.

$SiO_2$ consists of tetrahedra connected via the edges (Fig. 1a). One derives:

$$s_{Si} = \frac{+4}{4} = +1; \quad s_O = \frac{-2}{2} = -1$$

$$\zeta_{Si} = 4 \times (-1) = -4; \quad \zeta_O = 2 \times 1 = 2$$

At the surface, sites are created where one $Si^{4+}$ cation becomes surrounded by three $O^{2-}$ anions, and where $O^{2-}$ remains adsorbed to the $SiO_4$ tetrahedron, but loses the other $Si^{4+}$ neighbour. This implies that:

$$v^+ = +1$$

$$v^- = -1$$

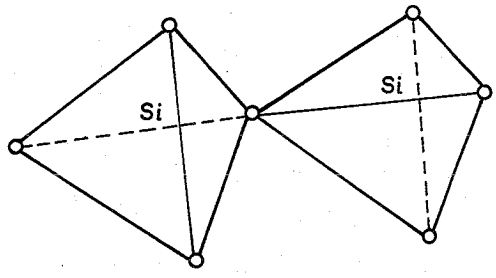


*Fig. 1a. $SiO_2$ tetrahedra.*

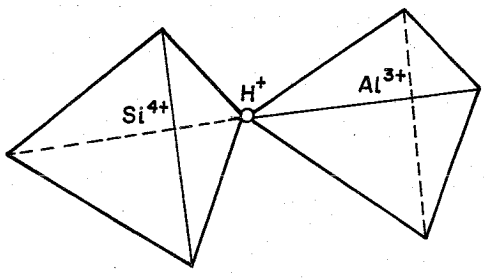


*Fig. 1b. $SiO_2/AlO_2^-$ tetrahedra in a zeolite.*

So the dehydrated silica surface is, according to *Pauling*'s electrostatic valence rule, more highly Lewis acidic and basic than dehydrated alumina. Upon hydration the Lewis acidic $Si^{4+}$ cations become coordinatively saturated because of adsorption of an $OH^-$ ion. A proton adsorbs to coordinatively unsaturated $O^{2-}$. So the unsaturated valencies become:

$$v^+ = v^- = 0$$

Thus, the surface silanol groups are only weakly acidic and basic. These qualitative predictions agree with the experimentally found differences between $Al_2O_3$ and $SiO_2$ surfaces[4].

Zeolites are silica aluminates that behave as strong solid acids. The crystals are built from tetrahedra as in $SiO_2$, but with $Si^{4+}$ partly replaced by $Al^{3+}$. The negative charge created is compensated by adsorbed cations positioned in cages and channels formed in the zeolite crystal. In case protons are used as cation the material behaves strongly acidic. Using *Pauling*'s electrostatic valencies this is readily explained, since the $v^-$ of the oxygen ions bonded to $H^+$, $Si^{4+}$ and $Al^{3+}$ (see Fig. 1b) is found to be:

$$v^- = +\frac{3}{4}$$

[4] *K. Tanabe*, "Solid Acids and Bases", Kodanska, Academic Press, 1970; *Ch. L. Thomas*, Ind. & Eng. Chem. **41**, 2566 (1949); *K. Tanabe, T. Sumiyoshi, K. Shibata, T. Kiyoura* and *J. Kitagana*, Bull. Chem. Soc. Japan **47** (5), 1064 (1974).

[5] Calculations done by J. Woning of our Laboratory.

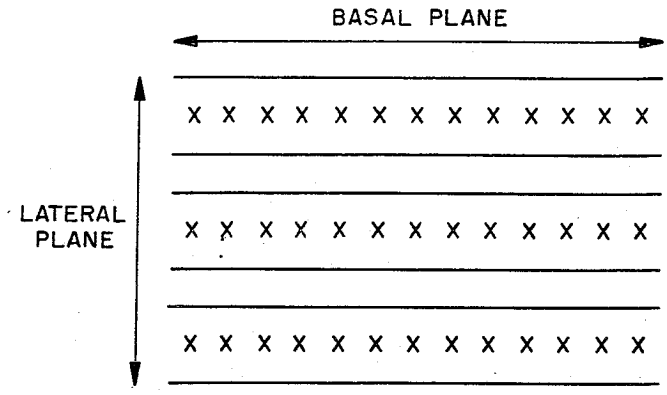


*Fig. 2. Schematic representation of the layers in a smectite: tetrahedral layer ———— ; octahedral layer × × × × ×.*

Not only in zeolites but also in clays acidic sites created by substitution of $Al^{3+}$ into $SiO_4$ tetrahedra are found. This is rather interesting since these turn out to be of low acidity. Clearly this means that a purely local approach as is implicit in the use of *Pauling*'s electrovalencies has to be modified so as to include differences in potential due to the structure of the crystal.

As illustration of the effects to be expected, in Table I differences in Madelung potential for two faces of rutile are presented[5]. The calculations have been performed for the (100) and (110) faces of $TiO_2$.

At the (100) face $Ti^{4+}$ is four-coordinated. According to *Pauling*'s rule $v^+(100)$:

$$v^+(100) = +\frac{4}{3}$$

Each oxygen ion has two $Ti^{4+}$ ions as neighbour at the (100) face, so that

$$v^-(100) = -\frac{2}{3}$$

Since the surface contains 2 $O^{2-}$ ions and one $Ti^{4+}$ ion charge neutrality is maintained.

*Table I Madelung potentials at $TiO_2$ (rutile) 100 and 110 faces[5] (unit Rydberg).*

| 100 face | | |
|---|---|---|
| $L$ | $\phi(Ti^{4+})$ | $\phi(O^{2-})$ |
| 0 | −2.8996 | 1.6284 |
| 1 | −3.3889 | 1.9190 |
| 2 | −3.2958 | 1.8808 |
| 3 | −3.3089 | 1.8829 |
| 4 | −3.3096 | 1.8801 |
| 5 | −3.3120 | 1.8780 |

| 110 face | | | | |
|---|---|---|---|---|
| $L$ | $\phi^1(Ti^{4+})$ | $\phi^2(Ti^{4+})$ | $\phi^1(O^{2-})$ | $\phi^2(O^{2-})$ |
| 0 | −2.2913 | −2.6754 | 2.0534 | 2.7262 |
| 1 | −2.5322 | −2.5167 | 2.6093 | 2.6629 |
| 2 | −2.5419 | −2.5424 | 2.6438 | 2.6480 |
| 3 | −2.5591 | −2.5589 | 2.6100 | 2.6289 |
| 4 | −2.5768 | −2.5766 | 2.5843 | 2.6133 |
| 5 | −2.5926 | −2.5925 | 2.6766 | 2.5975 |

At 100 face ($L = 0$) $Ti^{4+}$ is four-coordinated; $O^{2-}$ is two-coordinated.

At 110 face ($L = 0$) $Ti^{4+}$ five-coordinated, $\phi^1$ and six-coordinated $\phi^2$; $O^{2-}$ two-coordinated, $\phi^1$ and three-coordinated $\phi^2$.

At the (110) face one finds $Ti^{4+}$ ions, surrounded by six $O^{2-}$ ions and $Ti^{4+}$ ions coordinated to five $O^{2-}$ ions. For the latter $Ti^{4+}$ ion:

$$v_5^+(110) = +\frac{2}{3}$$

There are two kinds of $O^{2-}$ anions at the surface: three- and two-coordinated to $Ti^{4+}$. The latter $O^{2-}$ has $v^-$ equal to $-\frac{2}{3}$.

The results of the electrostatic potential ($\phi$) calculations presented in Table I show indeed a change in electrostatic potential between bulk and surface ions. The differences extend only over a few atomic distances.

At the (110) face differences in potential agree with expectations. The $\phi(Ti^{4+})$ of $Ti^{4+}$ that is six-coordinated at the surface is less than in the bulk, indicating the effect of changes in the environment of the octahedron. A similar result is found for the three-coordinated $O^{2-}$ ions. The decrease in potentials of $Ti^{4+}$ that is five-coordinated and $O^{2-}$ that is two-coordinated is larger, but less than predicted by *Pauling*'s rule.

Whereas $v^+(100) > v_5^+(110)$ according to *Pauling*, the differences between surface potentials of $Ti^{4+}$ at the (110) and the (100) face do not follow this rule. This is due to the finite dipole moment on the (110) face. As a result of this dipole moment the potentials in the bulk bounded by the (110) face, differ by a constant value from that found for bulk atoms bounded by the dipole-less (100) face. This does not affect the cohesive energy since this is related to $\phi(Ti^{4+})-\phi(O^{2-})$, which indeed is found to be equal for both cases (Table II). Even after correcting for the dipole layer potential, the degree of coordination does not follow the same order as that predicted using *Pauling*'s rule. According to the calculation the combination of five-coordinated $Ti^{4+}$ and two-coordinated $O^{2-}$ at the (110) face is more reactive than four-coordinated $Ti^{4+}$ and two-coordinated $O^{2-}$ at the (100) face.

Consequently this simple model predicts that $H_2O$ should be stronger adsorbed to these sites on the (110) face than to the (100) face of rutile. This result illustrates similar results to be presented below for some clays. If one accounts properly for the three-dimensional structure of an ionogenic surface, prediction different than using *Pauling*'s rule are sometimes found.

Not withstanding the very crude approximations involved, *e.g.* neglect of polarization and surface rearrangement, we will show for the case of clays that electrostatic calculations incorporating details of the matrix containing the catalytically active site lead to agreement with experimental results presented.

## 2. Some experimental results; the Ni–SMM clay

Of course, the method to measure surface acidity defines its meaning. A catalytic experiment useful to determine the acidity of a material is the hydroisomerization of alkanes. On the solid-acid catalyst to be discussed here alkanes are isomerized via a bifunctional mechanism[6]. A small amount of a noble metal (0.1–0.5 %w) is dispersed on the catalyst, so that hydrogenation and dehydrogenation reactions rapidly occur.

The acidic protons protonate alkenes, so that carbenium ions become adsorbed to the oxide surface. The slow step is the rate of protonation or the rate of isomerization of the carbenium ions.

A solid acid is stronger in the catalytic sense when the reaction attains a particular rate at a lower temperature. Differences in number of protons cause much smaller effects than differences in intrinsic acidity, which is of our concern here.

Table III presents a list with such temperatures determined under comparable conditions for different synthetic clays studied for $C_5$ isomerization. In addition the isomerization temperature for a sample of the zeolite Mordenite[7] is presented.

The clays used all belong to the class of the smectites. Their activities are, except for the Ni–SMM clay, appreciably smaller than those of the zeolites.

This class of clays consists of three-layer sheets stacked parallel to each other[13], as shown schematically in Fig. 2. Each three-layer sheet consists of one layer containing oxygen octahedra sandwiched between two layers containing oxygen tetrahedra. The basic structure contains $Si^{4+}$ cations in the centres of tetrahedra and $Al^{3+}$ ions in the centres of octahedra. The Si/Al ratio then is 2.

[6] *H. L. Coonradt* and *W. E. Garwood*, Ind. Eng. Chem., Prod. Res. Dev. **3**, 308 (1964); *J. Weitkamp*, Erdöl–Kohle–Erdgas, Petrochem.–Brennstof. Chem. **25**, 494 (1972).

[7] *P. B. Korodia, J. R. Kiovsky* and *M. G. Asim*, J. Catal. **66**, 290 (1980).

[13] *R. M. Barrer*, "Zeolites and Clay Minerals as Sorbents and Molecular Sieves", Academic Press, 1978.

*Table II Madelung potential differences at $TiO_2$ (rutile) 100 and 110 faces (unit Rydberg).*

| 100 face | |
|---|---|
| *L* | $\phi(Ti^{3+})-\phi(O^{2-})$ |
| 0 | 4.5280 |
| 1 | 5.3079 |
| 2 | 5.1760 |
| 3 | 5.1918 |
| 4 | 5.1897 |
| 5 | 5.1900 |

| 110 face | | | | |
|---|---|---|---|---|
| *L* | $\phi^1(Ti^{4+})-\phi^1(O^{2-})$ | $\phi^1(Ti^{4+})-\phi^2(O^{2-})$ | $\phi^2(Ti^{4+})-\phi^1(O^{2-})$ | $\phi^2(Ti^{4+})-\phi^2(O^{2-})$ |
| 0 | 4.3447 | 5.0175 | 4.7288 | 5.4017 |
| 1 | 5.1415 | 5.1951 | 5.1260 | 5.1796 |
| 2 | 5.1980 | 5.1899 | 5.1862 | 5.1904 |
| 3 | 5.1691 | 5.1888 | 5.1689 | 5.1878 |
| 4 | 5.1611 | 5.1901 | 5.1608 | 5.1899 |
| 5 | 5.1692 | 5.1901 | 5.1691 | 5.1900 |

*Table III Comparison of the activities of some clays.*

| Clay[8] | Temp. (°C) | Conversion | $k^{350}$ (°C)[c] (g/g h) |
|---|---|---|---|
| Hectorite-H[a] | 403 | 2 | $2 \times 10^{-4}$ |
| Beidellite-H[a] | 285 | 2 | $8 \times 10^{-3}$ |
| Ni–SMM-H[a] | 250 | 55 | 2.133 |
| Zeolite | – | – | – |
| Mordenite-H[7 b] | 260 | 55 | 0.73 |

Stoichiometry: Hectorite-H

$$(Si_8)\,(Mg_{5.22}Li_{0.48})O_{20}OH_{2.5}F_{1.5}$$

Stoichiometry: Beidellite-H

$$(Si_{5.78}Al_{2.22})Al_4O_{20}OH_{2.5}F_{1.5}$$

Stoichiometry: Ni–SMM-H

$$(Si_{5.26}Al_{2.74})\,(Al_{1.32}Ni_{4.02})O_{20}OH_{2.5}F_{1.5}$$

Stoichiometry: Mordenite-H

$$(SiO_2/Al_2O_3 = 17)$$

[a] %w Pd: 0.7; suface area 150 $m^2/g$; WHSV = 2 g/g h; $H_2/C_5$ = 1.25.

[b] %w Pd: 0.5; LHSV = 1 ml/ml h; $H_2/C_5$ = 1.81.

[c] Calculated rate of $C_5$ conversion at 250°C, $E_{act}$ = 25 kcal/mol.

One third of the octahedra is unoccupied so that charge neutrality is maintained. A top view of the beidellite structure is given in Fig. 3a, a side view in Fig. 3b. A clay in this form has only acidic sites in the lateral plane, where the lattice is disrupted. The sites are only weakly acidic since the tetrahedra are terminated by the formation of silanol groups.

The clay can be made acidic in several ways. One way is to replace some $Si^{4+}$ ions by $Al^{3+}$ ions in the tetrahedra and use protons as cations adsorbed on the lateral plane and within the spacing between the three sheet layers to compensate for the negative charges created. These acidic sites have the same local site geometry as protons in a zeolite, but clearly their acidity is much lower (beidellite-H).

It should be noted that because the catalyst has been calcined the hydroisomerization activity is limited to the lateral and basal planes.

A highly acidic clay is the so-called Ni–SMM clay[9] (SMM = Substituted Mica Montmorillonite). It consists of beidellite-H, but with part of the $Al^{3+}$ ions in the octahedral layer replaced by $Ni^{2+}$ ions. Substitution is such that three $Ni^{2+}$ ions replace two $Al^{3+}$ ions, so that electroneutrality is preserved.

From pyridine poisoning experiments and Fourier Transform-Infrared (FT-IR) measurements[10], it can be concluded that this increased activity is due to the increased acidity of the Ni–SMM clay caused by reduction of Ni[11].

Fig. 4 shows the effect of pyridine poisoning on the conversion of methylcyclopentane (MCP). Under the conditions applied, the main reaction of MCP is isomerization to cyclohexane (CH). In addition it can undergo ring opening, which may be either acid-catalysed or metal-catalysed. The initial CH/(CH + MCP) ratio shown indicates that isomerization conversion is at equilibrium.

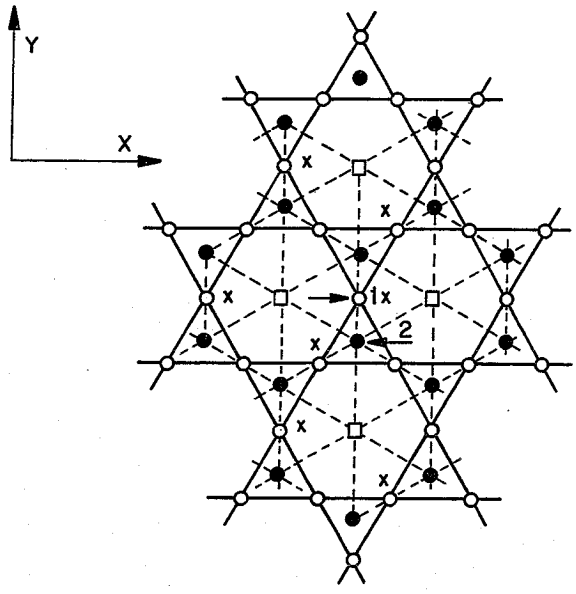


FIG. 3a

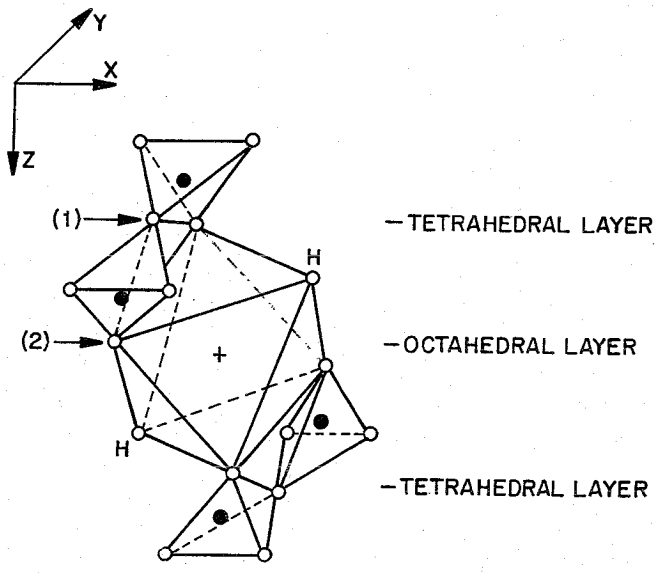


FIG. 3b

*Fig. 3. Structure of smectite. Arrows denote oxygen positions whose electrostatic potential has been calculated.*

*a.* x,y *plane, top view:*

——— *plane of oxygen atoms* z = *0;*

– – – – – *plane of oxygen atoms* z = *2.171 Å;*

○ *oxygen ions,* z = *0;*

● *Si ions,* z = *0.553 Å; atoms* z = *2.171 Å;*

□ *$OH^-$ ions,* z*($O^{2-}$)* = *2.171 Å;*

× *Al ions,* z = *3.50 Å.*

*b. Side view.*

The second class of products formed consists of about 4% hexanes resulting from ring opening. Isomerization is totally and irreversibly poisoned by means of several pyridine pulses, whereas ring opening goes through a minimum and reaches the former level again when poisoning is discontinued. Therefore it is concluded that MCP ring opening over Ni–SMM is catalysed by the metal sites, which are only reversibly poisoned by pyridine, while isomerization is catalysed by the acidic sites, which are

[8] Experiments done by J. Gaaf of our Laboratory.

[9] *H. E. Swift* and *E. R. Black*, Ind. Eng. Chem., Prod. Res. Dev. **13**, 106 (1974).

[10] *C. H. Röbschläger, C. H. Emeis* and *R. A. van Santen*, J. Catal., submitted for publication.

[11] *J. J. Heinerman, J. Gaaf, G. T. Pott* and *J. C. T. Coolegem*, J. Catal., submitted for publication.

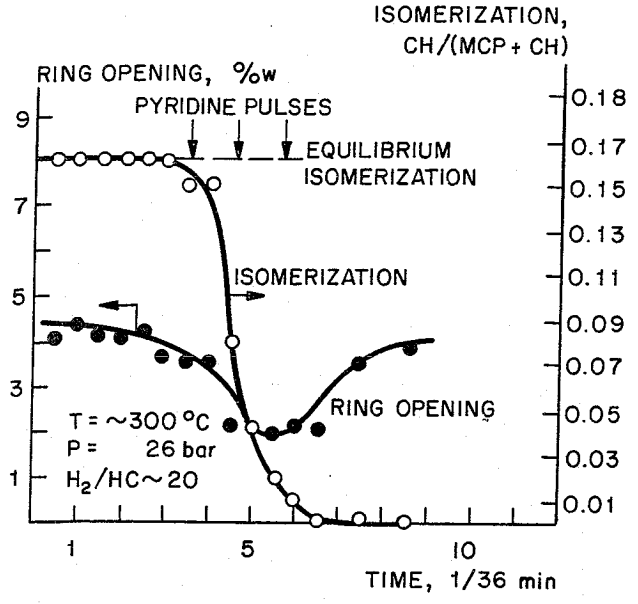


*Fig. 4. Effect of pyridine on the conversion of MCP.*

irreversibly poisoned by pyridine. So the high activity of Ni–SMM must be due to its strong acidic function.

The results of the FT-IR investigations using pyridine adsorption are shown in Figs. 5 and 6. A briefly calcined (4 h at 540°C) sample of Ni–SMM (0.7 %w Pd, 27.5 %w Ni) was used. As shown in Fig. 5, after admission of pyridine and pumping at 20°C the Ni–SMM contained pyridine bound to Brønsted acidic sites (NH bending mode of the pyridinium ion at 1550 $cm^{-1}$) and the weakly acidic Lewis sites (ring vibration at 1613 $cm^{-1}$). The relative amounts of pyridine that desorbed on pumping for 1 h at 150, 250 and 400°C are given in Fig. 6. Desorption was almost complete at 400°C. *In-situ* reduction (1 bar $H_2$ at 300°C for 16 h) resulted in a spectrum after pyridine adsorption (see Fig. 6b), which showed five times as many Brønsted sites as before reduction (compare the 1550 $cm^{-1}$ band in Fig. 6a). The number of Lewis acid sites had remained constant, but their average strength had increased. The desorption experiments show that the newly formed Brønsted sites are strongly acidic (see Fig. 6b).

The FT-IR experiments show clearly that the increase in acidity is due to an increase of the number of protons of high intrinsic acidity. There are two possibilities: Firstly, the protons created by $Ni^{2+}$ reduction are solely coordinated to the tetrahedra and are located in the basal plane. These protons are compensated by a negative charge located in the octahedral layer at the reduced $Ni^{2+}$ positions. Secondly, the protons produced are located in the octahedral layer.

The first possibility has been checked by hydroisomerization tests with synthetic hectorite exchanged into the acidic form (see Table IV). In hectorite no $Al^{3+}$ is present in the tetrahedral layer. Negative charge is created in the octahedral layer by substitution of $Li^{+}$ for $Al^{3+}$. This negative charge is compensated in hectorite-H by protons on the lateral plane. The activity of hectorite-H is found to be very low. So the second possibility appears the more likely.

## 3. Electrostatic model calculations

Using *Evjen*'s method[12] we have done approximate electrostatic calculations incorporating effects due to the structure of the lattice to which the protons are bonded. In *Evjen*'s method the charges on the atoms that bound the cluster of atoms used in the calculations are equal to the bulk charge, but are corrected for the missing bond strengths calculated according to *Pauling*'s electrostatic valence rule.

[12] *H. H. Evjen*, Phys. Rev. **39**, 675 (1932).

*Table IV Madelung potentials ϕ (unit Rydberg).*
$r_{cat\text{-}anion} = 1.61$ Å; $r_{an\text{-}anion} = 2.65$ Å.
$\Delta = \phi(O^{2-}) - \phi(H^{+})$.

| Ion structure | | $O^{2-}$ | $H^{+}$ on 1 Å in channel | $H^{+}$ on 1 Å in wall of channel |
|---|---|---|---|---|
| Mordenite | ϕ | 4.05 | −0.79 | −0.22 |
| | Δ | | 4.84 | 4.27 |
| Smectite | | | | |
| Tetrahedral position 1 | | | $H^{+}$ on 1 Å perp. to lat. plane | $H^{+}$ on 1 Å in lat. plane |
| Beidellite-H | ϕ | 1.68 | −1.78 | −1.58 |
| | Δ | – | 3.46 | 3.26 |
| Reduce 1 $Ni^{2+}$ Remove 2 $OH^{-}$ | ϕ | 1.29 | −1.92 | – |
| | Δ | – | 3.13 | – |
| Hectorite-H | ϕ | 1.56 | −1.71 | – |
| | Δ | – | 3.27 | – |
| Morillonite-H | ϕ | 1.95 | −1.51 | – |
| | Δ | – | 3.46 | – |
| Octahedral position 2 | | | $H^{+}$ on 1 Å in *y* dir. | $H^{+}$ on 1 Å in *x* dir. |
| Beidellite-H | ϕ | 2.26 | −0.22 | −0.24 |
| | Δ | – | 2.48 | 2.50 |
| 1 $Ni^{2+}$, 1 $Al^{3+}$ in oct. pos. around position 2 | ϕ | 2.70 | – | – |
| Reduce 1 $Ni^{2+}$, remove 1 $OH^{-}$ | ϕ | 3.25 | −0.551 | −0.762 |
| 1 $Ni^{2+}$ (non-reduced) + 1 $Al^{3+}$ in oct. pos. | Δ | – | 3.80 | 4.01 |

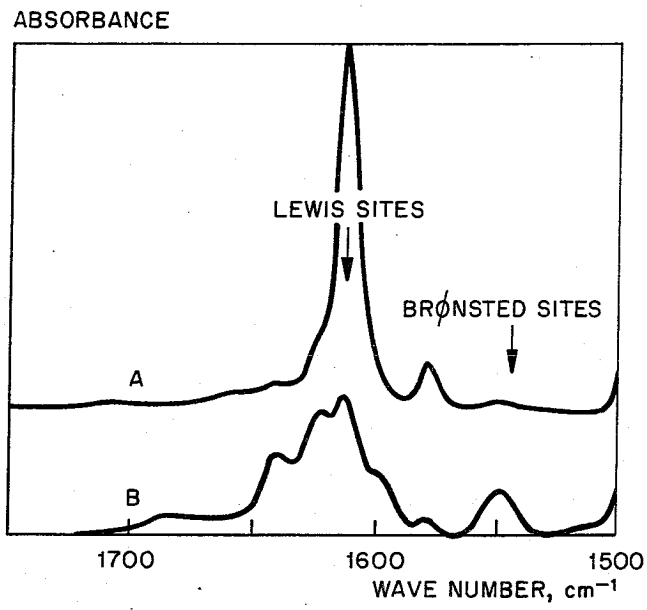


*Fig. 5. Infrared spectra of pyridine adsorbed by Ni–SMM. A: Before reduction. B: After reduction.*

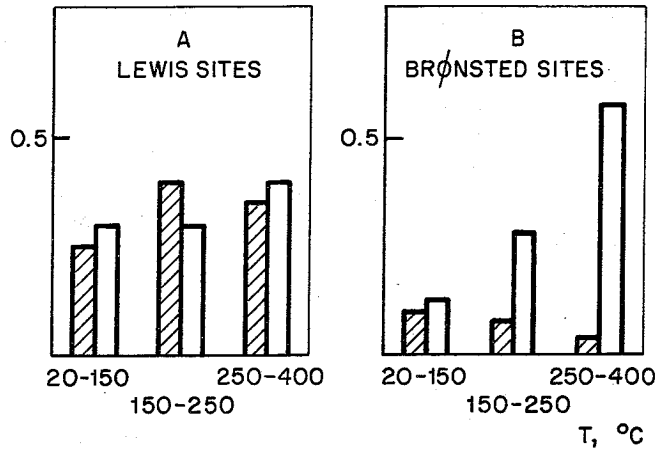


*Fig. 6. Amount of pyridine desorbed from Ni–SMM prior to reduction (shaded bars) and after reduction (not shaded). A: From Lewis sites, relative to total amount of Lewis sites. B: From Brønsted sites, relative to total amount of Brønsted sites after reduction.*

In the calculation for mordenite 64 atoms have been included and for the smectite clays 97 atoms, excluding the protons. Fig. 7 shows the oxygen position in the mordenite channel for which the potential has been calculated. Fig. 3 does this for the smectite clay. Position 1 connecting two tetrahedra has, according to *Pauling*'s electrostatic valence rule, an acidity comparable with that of the zeolite. Table IV gives the calculated Madelung potentials at the $O^{2-}$ positions and positions of the proton or protonated species at a distance 1 Å* from the oxygen ion.

Comparison of the figures calculated for mordenite and beidellite (tetrahedral position 1) reveals that the potential at the $O^{2-}$ ion is much lower in beidellite than in mordenite. Of course, the negative potentials at the proton position are now larger. This higher negative potential at the clay surface stems from the dipole moment perpendicular to the basal plane due to the parallel orientation of the $SiO_2$ tetrahedra.

We can use the calculated figures to derive a measure for the acidity of the solid while realizing that we are basically interested in protonation energies. As mentioned in the introduction the protonation energy can be considered to have three components:

$$E_{\text{proton}} = E_{\text{solv}} + E_{\text{add}} - E_{\text{diss}}$$

where $E_{\text{diss}}$ is the energy cost of dissociating the –OH bond, $E_{\text{add}}$ is the energy gain of protonating a nucleophilic molecule and $E_{\text{solv}}$ is the solvation energy of the resulting carbenium ion due to its adsorption onto the ionized solid acid surface. Since in our comparisons $E_{\text{add}}$ can be considered constant, we have to determine a measure for $E_{\text{solv}} - E_{\text{diss}}$.

$E_{\text{diss}}$ is related to the potential at the $H^+$ position, $\phi(H^+)$. The protonated molecule will adsorb to the ionized surface at a position different from the original $H^+$ position. So $E_{\text{solv}} - E_{\text{diss}}$ is related to the potential difference of a positive charge between different positions on the ionized surface. $E_{\text{diss}}$ is also related to the potential at the $O^{2-}$ position, since the change in electric field at the $O^{2-}$ position determines the polarization energy gain, when $H^+$ is removed. At the site where the carbenium ion readsorbs polarization energy is lost, resulting in partial compensation of this term. The potential at the $O^{2-}$ site plays a role as well, since in the process of protonation charge is removed from between oxygen and hydrogen onto oxygen.

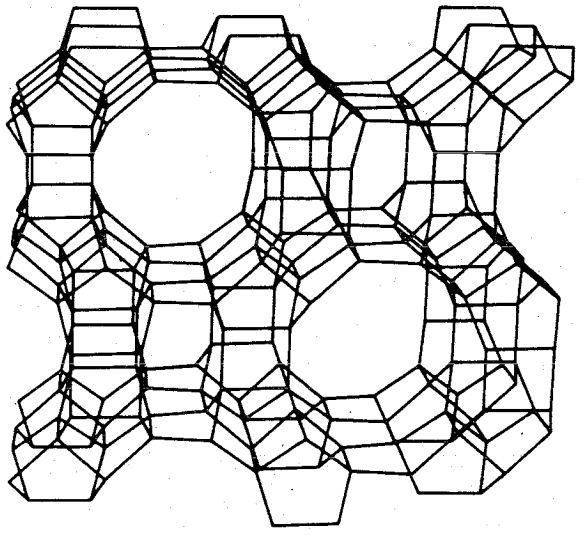

*Fig. 7a. Stereographic drawing of Mordenite channel*[14].

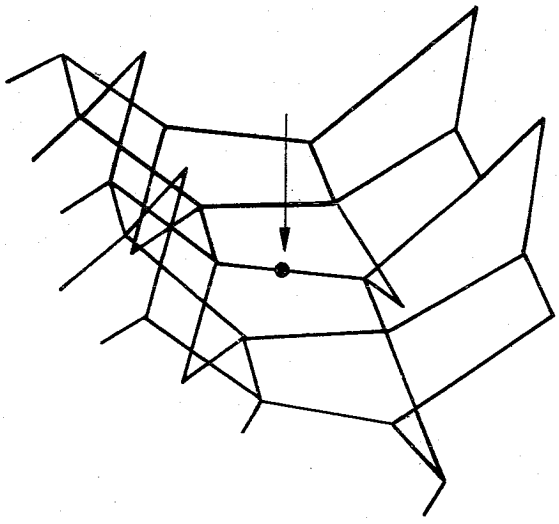

*Fig. 7b. Part of the channel and oxygen position (arrow), used in the electrostatic potential calculation of Mordenite.*

* 1 Å = 0.1 nm.

[14] *W. M. Meier* and *D. H. Olson*, "Atlas of Zeolite Structure Types", Polycrystal Book Service, 1978.

Thus, we arrive at a reasonable albeit very crude measure:

$$\Delta = \phi(O^{2-}) - \phi(H^{+})$$

As the table shows, the value of $\Delta$ is considerably higher for mordenite than for beidellite. This indicates that $\Delta$ may be a reasonable parameter.

In Ni–SMM $Ni^{2+}$ is partly substituted for $Al^{3+}$ in the octahedral layer. Substitution is such that charge neutrality in the octahedral layer is maintained, so two $Al^{3+}$ are replaced by three $Ni^{2+}$ ions. As a result one will find oxygen ions in position 2 of Ni–SMM surrounded by two $Ni^{2+}$ ions and one $Al^{3+}$ ion in the octahedral layer (configuration I) or by one $Ni^{2+}$ and one $Al^{3+}$ in the octahedral layer (configuration II). In configuration I we find $v^{-} = +\frac{1}{6}$ and in configuration II we have $-\frac{1}{6}$. According to *Pauling*'s electrostatic valence rule such deviations from zero do not lead to unstable minerals[3].

Reduction of one $Ni^{2+}$ and attachment of a proton to the oxygen ion in position 2 gives $v^{-} = +\frac{5}{6}$ in configuration I and $v^{-} = +\frac{1}{2}$ in configuration II. So application of *Pauling*'s electrostatic valence rule predicts an increase of weakly and strongly acidic sites at positions 2 upon reduction of Ni–SMM.

Since the example of beidellite indicates that in a clay the acidity is much weaker than expected from a calculation based on *Pauling*'s electrostatic valencies, we have included in Table IV values of $\Delta$ for Ni–SMM on position 1 after reduction and position 2 before and after reduction. We have also included the $\Delta$ values calculated for hectorite-H and montmorillonite-H at position 1. In hectorite-H some $Al^{3+}$ in the octahedral positions is replaced by $Li^{+}$. In montmorillonite-H some $Al^{3+}$ in the octahedral positions is replaced by $Mg^{2+}$. The resulting negative charges are in both clays compensated by protons in the lateral plane on or between the three-layer sheets. No $Al^{3+}$ is present in tetrahedral positions.

In agreement with experiment the $\Delta$ values calculated for montmorillonite and hectorite are low. The low value of $\Delta$ on position 1 for reduced Ni–SMM confirms the hypothesis that at this position no increase of acidity occurs.

The calculations done for position 2 show that an imaginary proton near that position in Ni–SMM is of lower acidity than the protons near position 1. Only after reduction does one find a value $\Delta$ that shifts into the direction of the value found for mordenite.

Thus the electrostatic calculations confirm that the increase in acidity of Ni–SMM is due to the creation of acidic sites in the octahedral plane. Therefore the catalytically active sites will be located in the lateral plane or edges of the clay.

Of course, the discussion presented so far is of a qualitative nature due to the particular choice of the parameter $\Delta$, but also due to limitations of *Evjen*'s method and neglect of polarization energy, which will make a significant contribution particularly at the boundaries of oxides. Besides, we have assumed that the distances in the clay remain unchanged upon substitution and that no surface rearrangement occurs.

A more rigorous approach is welcome, not only because it would improve the theory quantitatively, but also because it would indicate how the carbenium ions become adsorbed to the ionized surface.

Conclusions comparable to ours can be drawn from the work of *Mortier*[15], who studied differences of acidity between different zeolites. *Kasanski* and co-workers and others[16] using quantum-chemical methods have also found effects due to substitutional changes in tetrahedra located in the second coordination sphere.

---

[15] *J. Mortier*, J. Catal. **55**, 138 (1978); *P. A. Jacobs*, "Carboniogenic Activity of Zeolites", Elsevier, 1972.

[16] *I. D. Mikheikin, A. I. Lumpov, G. M. Zhidomirov* and *V. B. Kasanksi*, Kinet. Katal. **19**, 1053 (1978); *H. H. Dunken* and *R. Hoffman*, Phys. Chem. N.F. **125**, 207 (1981).